Structural Engineering and Mechanics, *Vol. 63, No. 4 (2017) 447-456*
DOI: https://doi.org/10.12989/sem.2017.63.4.447

Shear behavior of RC beams externally strengthened and anchored with CFRP composites

Rajai Z. Al-Rousan*

Department of Civil Engineering, Jordan University of Science and Technology, Irbid, Jordan

(Received January 4, 2017, Revised May 5, 2017, Accepted May 13, 2017)

Abstract. The primary objective of this paper is to study the effectiveness of anchorage on the performance of shear deficient beams externally strengthened with CFRP composites. The overall behavior of the tested beams loaded up to failure, the onset of the cracking, and crack development with increased load and ductility were described. The use of CFRP composites is an effective technique to enhance the shear capacity of RC beams by using CFRP strips anchored into the tension side and from the top by 15-34% based on the investigated variables. Bonded anchorage of CFRP strips with width of 0.1h-0.3h to the beam resulted in a decrease in average interface bond stress and an increase in the effective strain of the FRP sheet at failure, which resulted in a higher shear capacity as compared with that of the U-wrapped beams without anchorage as well as delay or mitigate the sheet debonding from the concrete surface.

Keywords: anchorage; shear behavior; RC beams; externally; strengthened; CFRP composites

1. Introduction

The deterioration of civil engineering infrastructures such as buildings, bridge decks, girders, offshore structures, parking structures are mainly due to ageing, poor maintenance, corrosion of steel reinforcement, defects in construction/design, demand in the increased service loads, exposure to harmful environments and damage in case of seismic events and improvement in the design guidelines. These deteriorated structures are deficient to take the load for which they are designed. A large number of structures constructed in the past using the older design codes in different parts of the globe are structurally unsafe according to the new design codes and hence need upgradation of the existing structures. Fiber-reinforced polymers (FRP) have emerged as promising material for rehabilitation of existing reinforced concrete structures and strengthening of the new civil engineering structures because of their several advantages such as high strength-to-weight ratio, high fatigue resistance, flexible nature, ease of handling, and excellent durability.

The use of external FRP strengthening to beams may be classified as flexural and shear strengthening. The shear failure of an RC beam is distinctly different from the flexural one in that the flexural is ductile in nature, whereas the shear one is brittle and catastrophic. When the RC beam is deficient in shear, or when its shear capacity is less than the flexural capacity after flexural strengthening, shear strengthening of the beam must be considered. It is critically important to examine the shear capacity of RC beams which are intended to be strengthened in flexure.

*Corresponding author, Ph.D.
E-mail: rzalrousan@just.edu.jo

The application of FRPs to strengthen the RC rectangular beams has received considerable attentions from the research community (Chaallal *et al*. 1998, Khalifa *et al*. 1998, Triantafillou 1998, Li *et al*. 2001, Khalifa and Nanni 2002, Pellegrino and Modena 2002, Chen and Teng 2003, Taljsten 2003, Teng *et al*. 2004, Cao *et al*. 2005, Zhang and Hsu 2005, Mosallam and Banerjee 2007, Sundarraja and Rajamohan 2009, Siddiqui 2009, Pannirselvam *et al*. 2009, Bukhari *et al*. 2010, Martinola *et al*. 2010, Ceroni 2010, Hosen *et al*. 2016, Hojatkashani and Kabir 2012, Anil *et al*. 2012, Shuraim 2011, Lee *et al*. 2008, Jayaprakash *et al*. 2007). However, only a few numbers of studies on the shear strengthening of RC T-beams with externally bonded FRPs are reported in the literature. Khalifa and Nanni (2000) studied the shear performance of RC T-beam strengthened with different configurations of externally bonded carbon FRP (CFRP) composites. Deniaud and Cheng (Deniaud and Cheng 2001) studied the interaction of concrete, steel stirrups, and external fiber-reinforced polymer (FRP) sheets in carrying shear loads in RC T-beams. Bousselham and Chaallal (2006) investigated the effect of the shear length to the beam depth ratio, the CFRP ratio and the internal transverse steel reinforcement ratio on the shear behaviour of RC T-beams. Also they (Bousselham and Chaallal 2008) investigated the shear resistance mechanisms in RC T-beams strengthened in shear with externally bonded FRP.

The most popular techniques based on the use of FRP reinforcements are the Externally Bonded Reinforcement (EBR) and the Near Surface Mounted (NSM). According to the EBR technique, sheets or laminates of carbon fiber reinforced polymers (CFRP) are bonded on the faces of the elements to be strengthened. In case of the NSM technique, CFRP laminates or bars are installed into slit/grooves sawed into the beams concrete cover and bonded to the concrete substrate by polymer adhesive. Due to the confinement

ISSN: 1225-4568 (Print), 1598-6217 (Online)

provided by the surrounding concrete and the higher laminate-concrete bond surface (Bilotta *et al*. 2011, Seo *et al*. 2012), the available experimental research showed that NSM is more effective than EBR for shear strengthening (Dias and Barros 2011, Dias and Barros 2012, Dias and Barros 2013). Other concerns regarding the use of EBR, apart from the relatively high cost of the FRP systems, are the susceptibility to fire and acts of vandalism, as well as the longer time needed to prepare the beam zones for the FRP bond. Maximum efficiency using composites material is obtained when the strengthening system is able to exploit its full tensional strain. Both EBR and NSM techniques rely on the stress transfer capacity between FRP and the concrete substrate. However, the latter is usually the most damaged part of the RC elements. Most of the experimental tests showed that the strengthened elements fail by debonding in EBR shear strengthening configurations. When using NSM technique the current failure modes are concrete fracture, followed by debond of the FRP systems. When the percentage of strengthening NSM-reinforcement is relatively high, the concrete cover including the FRP reinforcement has the tendency to detach due to the reasons explained elsewhere (Bianco *et al*. 2010). By applying the NSM technique, the full tensile capacity of the CFRP reinforcements can only be attained when these reinforcements are surrounded by relatively high strength concrete and bond transference length is assured (Dias and Barros 2013). A new strengthening technique, designated as Embedded Through-Section (ETS), has recently been investigated for the shear strengthening of RC beams (Valerio *et al*. 2009, Chaallal *et al*. 2011). According to this technique, steel or FRP bars are inserted into holes bored through the cross section and bonded with an epoxy adhesive. This technique can be more effective for the shear strengthening due to the higher confinement provided by the concrete surrounding the bars, and the larger concrete fracture surface that is mobilized during the pullout process applied to the ETS bars crossing the shear crack.

It is observed from the existing literature that the potential use of CFRP strips in strengthening the RC rectangular beams is reported, but not on the beams with anchorage to the best knowledge of the authors. There are limited works on shear strengthening of RC beams using mechanically anchored FRP sheets (Lee *et al*. 2011, Sato *et al*. 1997, Schuman 2004, Galal and Mofidi 2010, Mofidi *et al*. 2012). The primary role of FRP anchorage systems is to prevent or delay the process of debonding, which occurs when externally bonded FRP detaches from the RC substrate because of the low tensile strength of concrete. Anchorage systems are also used to provide a load transfer mechanism at critical locations of structural members or in some cases provide a ductile failure mode for the structural member instead of the typical sudden, brittle failure modes of FRP debonding and rupture. The performance of anchorage systems becomes critical in the design of FRP strengthening systems because they may limit the strength of the FRP system. Associated failure modes including global anchorage failure or FRP rupture due to local stress concentrations imposed by the anchorage are sudden and brittle in many situations; thus a thorough understanding of the behavior of anchorage systems is essential for a safe and reliable design. Based on the critical review of the existing literature, the main objective of the present work is to study the effect of anchorage on the shear behavior of RC beams externally strengthened with CFRP composites in term of mode of failure, load deflection behavior, CFRP maximum strain, concrete compression strain, steel tensile strain and crack opening.

Table 1 Mixture design proportions of concrete

Ingredients	Mix proportions (For 1 m^3)
Cement	357 Kg
Coarse aggregate	1026 Kg
Fine aggregate	645 Kg
Silica fume	18 Kg
Fly ash	71 Kg
Water	161 Kg
RB 1000 super plasticizer	90 fl oz
MB-VR Air-Entraining	15 fl oz
$f_C^{'}$ at 28 days	55 MPa

Table 2 Mechanical properties of CFRP

Property	Provided amount	Tested amount
Ultimate strength	4275 MPa	----
Design strength	3790 MPa	3920 MPa
Yielding modulus	228 GPa	231 GPa
Ultimate strain	0.0168 mm/mm	0.017 mm/mm
Thickness	0.165 mm	0.165 mm

2. Description of experimental program

2.1 Ingredient properties

2.1.1 Concrete

All the specimens were made from the same batch of normal weight concrete and conventional fabrication and curing techniques were used. The maximum size of coarse aggregate was 19 mm crushed limestone. Type I Portland cement and admixture were used for all concrete mixes. Table 1 shows the mixture design proportions of concrete used in this study. The concrete mix had a slump in the range of 75-125 mm. Twelve 150×300 mm concrete cylinders were cast along with each group and cured in the moisture room. The average compressive strength of concrete ($f_C^{'}$) was determined by testing standard concrete cylinders after 28 days.

2.1.2 Carbon fiber sheets

One type of carbon fiber sheets was used in the research program depending on the manufacturers. This type was the carbon fiber unidirectional sheet in the form of tow sheet. The carbon fiber products come in a wide of rolls of 500 mm that can be cut into appropriate lengths. The carbon fiber tow sheet is tested by using a special fixer to catch the fiber from both sides and one of these side is fixed and the

Table 3 The details, ultimate load and mode of failure of tested shear beams

Beam Designation	Type of Strengthening	Ultimate load, kN	Percentage of increase w.r.t control beam, %	Failure mode
B2.7N0	None	129.9	0	Shear failure followed by 33^o diagonal crack
B2.7U90STA0	Strip@ 90^o U-wrap without anchoring	149.0	15	Shear failure followed by 37^o diagonal crack, debonding of CFRP strips
B2.7U90STA1	Strip@ 90^o U-wrap with 25 mm CFRP top strips anchoring	157.5	21	Shear failure followed by 37^o diagonal crack, debonding of CFRP strips
B2.7U90STA2	Strip@ 90^o U-wrap with 50 mm CFRP top strips anchoring	166.8	28	Shear failure followed by 37^o diagonal crack, debonding of CFRP strips
B2.7U90STA3	Strip@ 90^o U-wrap with 75 mm CFRP top strips anchoring	174.4	34	Flexural failure followed by crushing of concrete in compression zone

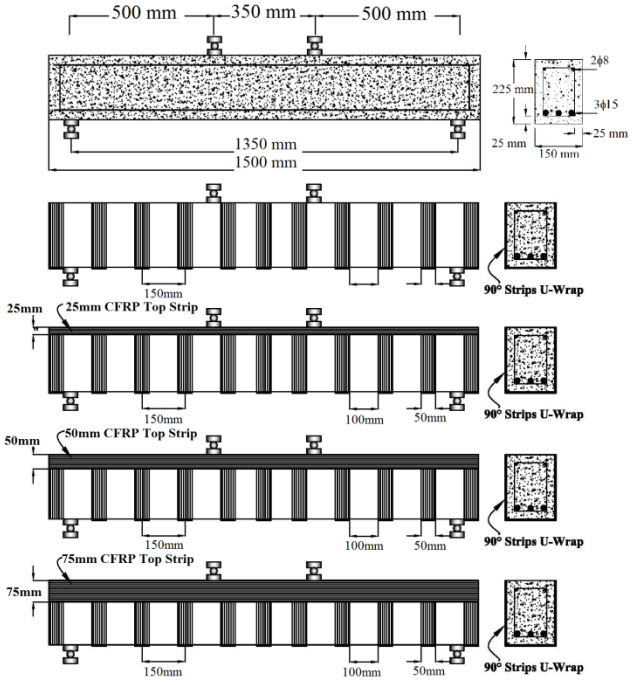

Fig. 1 Typical layout of the control and strengthened reinforced concrete shear beam

other moved down to apply a tension force in the tested specimen until the fracture of the carbon fiber. The provided and tested property of the carbon fiber tow sheet is shown in Table 2.

Before applying the carbon fiber, the concrete surfaces were roughen and treated to remove cement laitance, loose and friable material to achieve a profiled open textured surface, using wire brush on an electric drill. Dust was then removed using a vacuum cleaner, then the surface were brushed using thinner to clean the surface and reduce the moisture content.

2.2 Reinforced concrete beam details

Ten rectangular reinforced concrete beams, 150×225 mm with a total length of 1500 mm, were cast with the reinforcement of 2ϕ8 bars at the top and 3ϕ15 bars at the bottom and without stirrups for all the specimens. The design choices were made to ensure that shear failure would occur in the control beams and to measure the direct contribution of CFRP composite. The tested beams include: two beams were tested as control beams without strengthening, two strengthened beams without anchorage, two strengthened beams with 25 mm CFRP anchorage, two strengthened beams with 50 mm CFRP anchorage and two strengthened beams with 75 mm CFRP anchorage. The average value of the same tested beams will take as shown in Table 3. Fig. 1 shows the reinforcement and the CFRP strips configurations for all the beams. The main reason to choose the anchorage from the tope side is the mode of failure of strengthened beam without anchorage which is failed due to the debonding of CFRP strips from the top.

The CFRP sheets were applied to eight beams after 28 days of concrete casting. The CFRP sheets/strips of the required length were cut and bonded to the web face of the beams. The details and number of layers of carbon fiber for all beam specimens are shown in Table 3. In the beam designation of Table 3, the first letter "B" indicates the beam specimen, 2.7 stands for the shear span over effective depth (a/d). The letters: N stands for no strengthened; U90 for 90o U wrap, and ST for strip wrap. Finally, the letter, A0, stands for the anchoring followed by 1, 2, and 3 for the width of 25 mm, 50 mm, and 75 mm CFRP strips, respectively.

2.3 Test setup and instrumentations

All specimens were tested as simply supported in a special designed built-up rigid steel frame. A hydraulic jack was used to apply a concentrated load through a hydraulic cylinder on a spread steel beam to produce two-point loading condition to generate a constant moment region at mid-span. Before testing of the beams, the beams were simulated by using ANSYS package to determine the critical location of the maximum CFRP strain, crack opening, and deflection. Three types of instruments were used in the tests: linear variable differential transformers (LVDT), strain gages, and load cell. Five LVDTs were used, one to monitor the vertical displacement; the LVDT was located at mid-span, two to monitor the crack opening; the LVDT's were located at critical shear stress on both sides, one to monitor the strain at the steel level, and finally, one to measure the concrete strain at top face. For each specimen, at least four strain gages were attached directly to the compression face and critical shear zone of the beams to monitor the strain during loading; a strain gage was also embedded in side the beam to measure the strains in

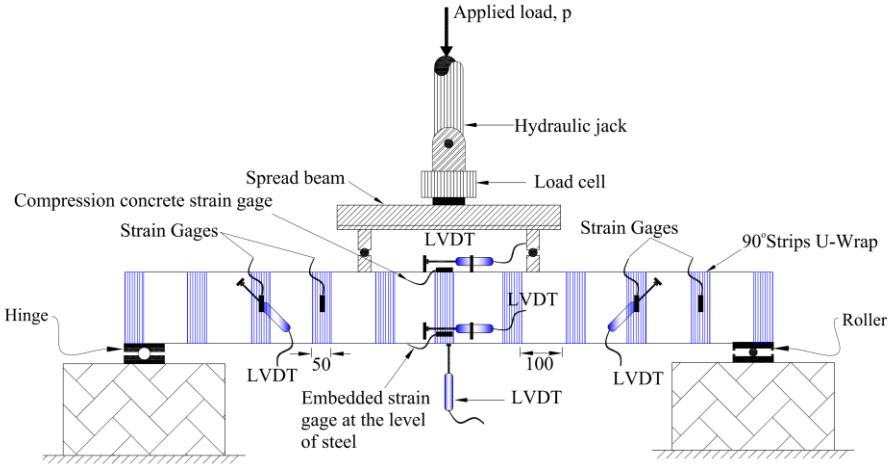

Fig. 2 Test set-up for reinforced concrete shear beams

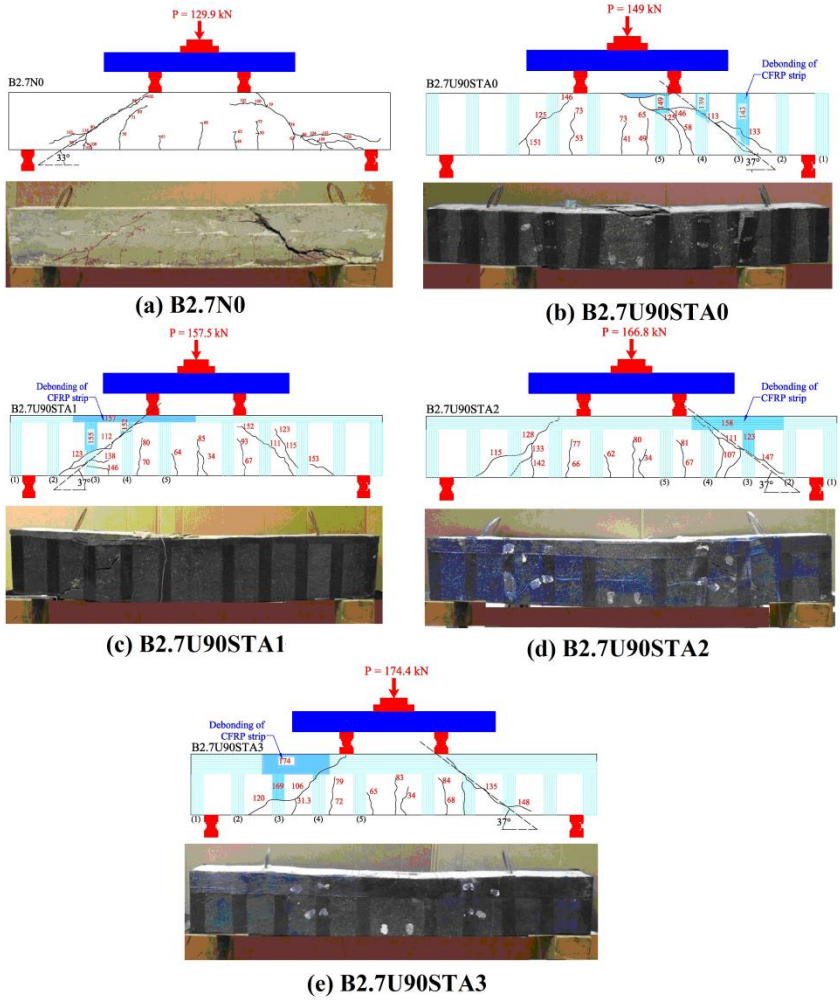

Fig. 3 A representative cracking patterns of tested beams

concrete at the level of steel before casting the specimens. A load cell was used to measure the applied load throughout the tests and a TDS 302 data acquisition system to collect the data of the strain gages, LVDTs, and the load. During loading, the formation of cracks on the sides of the beams were also marked and recorded. The reinforced concrete shear beam test set-up is shown in Fig. 2.

3. Experimental results and discussion

3.1 Mode of failure and ultimate load at failure

Fig. 3(a) shows the representative cracking pattern of B2.7N0. The initial flexural crack of control beam without reinforcement started at the center of the beam within the

constant moment region at 23.1 kN. Beyond this load, cracks extended toward the top fiber, and additional flexural cracks were developed throughout the beam length. At 77 kN, a 33-degree angle shear crack developed independently of the existing flexural cracks in the center of the shear span. With further load increase, the cracks extended both towards the support and the load point, leading to a sudden, brittle shear failure at 129.9 kN as shown in Fig. 3(a) and Table 3.

Fig. 3(b) shows the representative cracking pattern of B2.7U90STA0. The initial flexural crack started at the center of the beam within the constant moment region at 34.2 kN. Beyond this load, cracks extended toward the top fiber, and additional flexural cracks were developed throughout the beam length. At 112.5 kN, a 37-degree angle shear crack developed independently of the existing flexural cracks in the center of the shear span. With further load increase, the strip No. 4 was debonded at 139.2 kN followed by the debonded of strip No.3 at 142.8 kN. The beam failed successively at 149 kN after the debonding of strip No. 5 as shown in Fig. 3(b) and Table 3. Debonding of the CFRP strip is a delamination between the strip-adhesive-concrete at the strip-end region of the strengthened beam. This failure was a result of the maximum stresses in the adhesive being not greater than the bonding strength between strip-adhesive-concrete at the strip-end region.

Fig. 3(c) shows the representative cracking pattern of B2.7U90STA1. The initial flexural cracks started at the center of the beam within the constant moment region at 34.2 kN. Beyond this load, cracks extended toward the top fiber, and additional flexural cracks were developed throughout the beam length. At 112.1 kN, a 37-degree angle shear crack developed independently of the existing flexural cracks in the center of the shear span. With further load increase, Strip No. 4 was debonded at 151 kN followed by the debonding of Strip No. 3 at 161.5 kN. The beam failed successively in shear at 157.5 kN after the debonding of top anchoring strip over Strip No. 3, 4, and 5, respectively, as shown in Figure 3(c) and Table 3.

Fig. 3(d) shows the representative cracking pattern of B2.7U90STA2. The initial flexural crack started at the center of the beam within the constant moment region at 33.8 kN. Beyond this load, cracks extended toward the top fiber, and additional flexural cracks were developed throughout the beam length. At 115.6 kN, a 37-degree angle shear crack developed independently of the existing flexural cracks in the center of the shear span. With further load increase, Strip No. 4 was debonded at 124.5 kN followed by the debonding of Strip No. 3 at 140.1 kN. The beam failed successively in shear at 174.4 kN after the debonding of top anchoring strip over Strip No. 3 and 4, respectively, as shown in Fig. 3(d) and Table 3.

Fig. 3(e) shows the representative cracking pattern of B2.7U90STA2. The initial flexural crack started at the center of the beam within the constant moment region at 34.2 kN. Beyond this load, cracks extended toward the top fiber, and additional flexural cracks were developed throughout the beam length. At 112.5 kN, a 37-degree angle shear crack developed independently of the existing flexural cracks in the center of the shear span. With further load increase, Strip No. 4 was debonded at 169 kN followed by the debonding of Strip No. 3 at 173.9 kN. The beam failed successively in flexure at 174.4 kN after the debonding of top anchoring strip over Strip No. 3 and 4, respectively, as shown in Fig. 3(e) and Table 3.

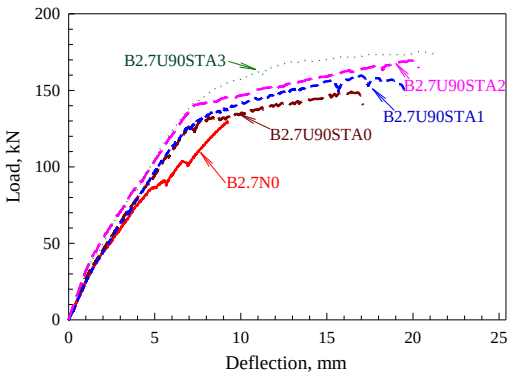

Fig. 4 Load-deflection curves for tested beams

3.2 Concrete strength results

Fig. 4 shows the load deflection curves for B2.7N0, B2.7U90STA0, B2.7U90STA1, B2.7U90STA2, and B2.7U90STA3. All strengthened beams exhibited almost relationships up to the load of 133.0 kN that equals to the failure load of control beam. This indicates that the CFRP started to carry the load after the formation of the diagonal shear. Inspection of Fig. 4 shows that the ultimate load capacity of the beams increased with the increase or anchoring system width as well as the increase in stiffness can be observed from the rotation angle of the elastic stage curve of the tested beams. In addition, Fig. 4 shows that the ultimate deflection at failure of the beam increased with the increase of anchoring system width which is the exact mirror of the mode of failure.

3.3 Concrete compressive strain

Fig. 5 shows the relationship between the load and concrete compressive strain for B2.7N0, B2.7U90STA0, B2.7U90STA1, B2.7U90STA2, and B2.7U90STA3 RC beams. The concrete compression strain increased with the increase in load. The corresponding loads for the compressive strain of 1150 με for B2.7N0, B2.7U90STA0, B2.7U90STA1, B2.7U90STA2, and B2.7U90STA3 were 118.3, 128.5, 130.3, 140.6, and 141.5 kN, respectively. This indicates that the compressive strain in the concrete decreases with the increase in the width of the anchoring system. The strengthened reinforced concrete beams with (B2.7U90STA3) CFRP sheet registered the highest strain. The load-compressive strain curves for tested RC beams indicated that B2.7U90STA3 beam registered a concrete strain more than 3000με.

3.4 CFRP tensile strain

Fig. 6 shows the relationship between the load and

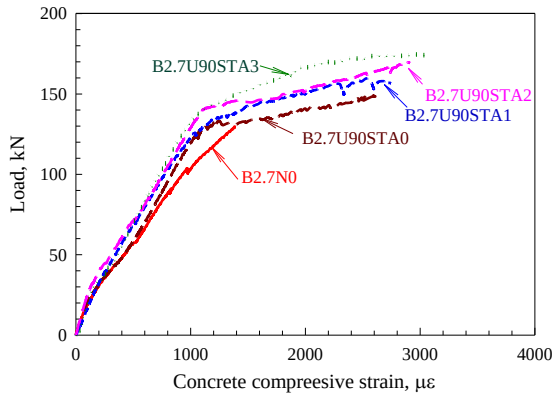

Fig. 5 Load-concrete compressive strain curves of tested beams

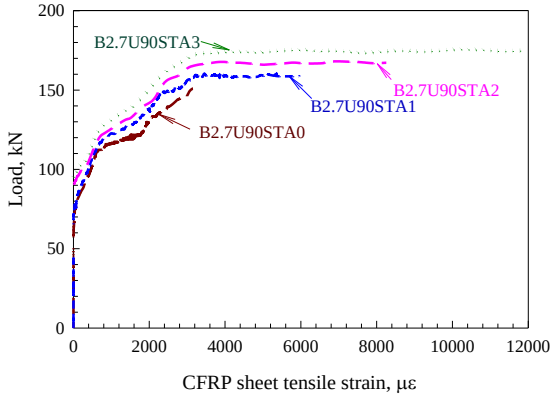

Fig. 6 Load-CFRP shear strips sheet tensile strain curve for tested beams

CFRP sheet tensile strain for B2.7U90STA0, B2.7U90STA1, B2.7U90STA2, and B2.7U90STA3 RC beams. Inspection of Fig. 6 reveals that the load-CFRP strain behavior of un-anchorage strengthened beam is almost linear after creation of the diagonal shear crack. While the load-CFRP strain behavior of anchorage strengthened beam is almost linear after creation of the diagonal shear crack up to 3000 ms then the curve changed to be straight up to failure of the beam. According to Fig. 6, the tension strain was initiated in the CFRP sheet after the diagonal shear crack started to formulate at loads of 77.0, 85.8, 85.2, 87.6, and 90.3 kN for B2.7N0, B2.7U90STA0, B2.7U90STA1, B2.7U90STA2, and B2.7U90STA3 beams, respectively. Fig. 6 also shows that the development of strains becomes sluggish around a load of 93.4 kN in all beams. Inspection of Fig. 6 reveals that the CFRP tensile sheet strain increased with the increase in the width of the anchorage system. From this, it is known that the development of strain is slower as the anchoring system width decrease. At ultimate load, the tensile strains were 3165, 5960, 8230, and 11800 με for B2.7U90STA0, B2.7U90STA1, B2.7U90STA2, and B2.7U90STA3 beams, respectively, which is equivalent to $0.19\varepsilon_{fu}$ (745 MPa), $0.35\varepsilon_{fu}$ (1372 MPa), $0.48\varepsilon_{fu}$ (1882 MPa), and $0.69\varepsilon_{fu}$ (2704 MPa), respectively. These higher strains of CFRP strips reflected the efficiency of the anchorage system in the strengthening of shear deficient beams. Therefore, the B2.7U90STA3 strengthened beam showed lower tensile strain than other strengthened beam for the same load. Finally, the CFRP strain value and mode of failure of tested beams show that the maximum strain is occurred in the middle point of strip No. 3 as shown in Fig. 3 and then decreased to reach zero strain at the bottom face of the beam because of no separation occurred at the bottom side of all CFRP strips. While higher stress distribution was occurred at the top side of the CFRP strips because of the failure of the CFRP anchorage above strip No. 3 and No. 4 and this delimitation decreased with the increase of anchorage CFRP width from 25 mm to 75 mm. This phenomenon reflects the efficiency of anchorage system in the increasing of the CFRP shear strip contribution and changing the failure from brittle shear failure to ductile flexural failure.

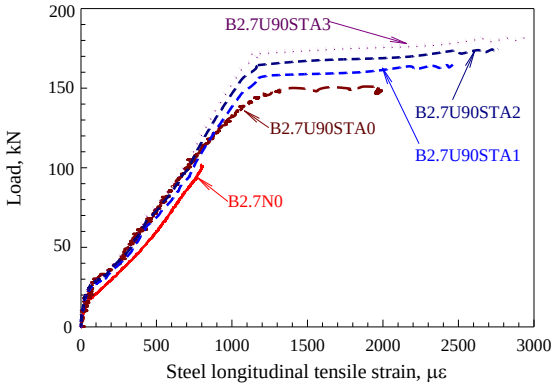

Fig. 7 Load- longitudinal steel tensile strain curves of tested beams

3.5 Steel tensile strain

Fig. 7 shows the relationship between the load and strain at the level of steel for B2.7N0, B2.7U90STA0, B2.7U90STA1, B2.7U90STA2, and B2.7U90STA3 RC beams. The load strain curve followed the same trend for all the beams before the cracking. After cracking the slope of the curve was reduced as a result of reduction in stiffness. Inspection of Fig. 7 reveals that the steel tensile strain followed the same trend and behavior as the concrete compressive strain which increased with increasing the load as well as the steel tensile strain in the concrete decreased with the increase in the width of the anchoring system. All the anchored beams reached the yielding point as well as the steel reinforcement in B2.7U90STA3 strengthened beam experienced highest tensile strain development than that of other beams at ultimate load.

3.6 Crack opening behavior

Fig. 8 shows the relationship between the load and crack opening for B2.7N0, B2.7U90STA0, B2.7U90STA1, B2.7U90STA2, and B2.7U90STA3 RC beams. According to Fig. 8, crack opening width started after the diagonal shear crack was initiated at load 77.0, 85.8, 85.2, 87.6, and 90.3 kN for B2.7N0, B2.7U90STA0, B2.7U90STA1, B2.7U90STA2, B2.7U90STA3, respectively, after the

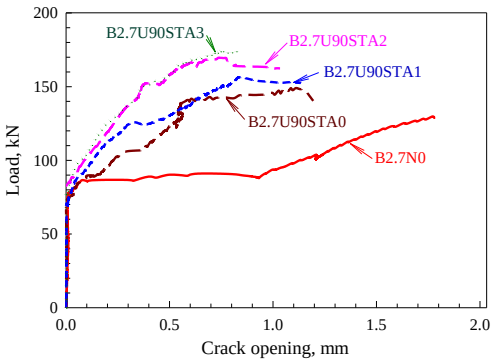

Fig. 8 Load crack opening curves for beams with different anchorage systems

formulation of diagonal shear crack. Fig. 8 shows also that the development of crack width also becomes sluggish around 0.25 mm in all beams. It can be observed the crack developed at a slower rate as the increase of anchoring system width. At ultimate load, the ultimate crack width is 1.78, 1.19, 1.12, 1.03, and 0.81 mm for B2.7N0, B2.7U90STA0, B2.7U90STA1, B2.7U90STA2, and B2.7U90STA3, respectively. Therefore, the B2.7U90STA3 strengthened beam showed less crack width for the same load than the other beams.

4. Comparison of experimental results with analytical models

For purposes of comparison, tested results are compared with those of the ACI model (ACI 2008), Triantafillou model (Triantafillou 1998), and Colotti *et al*. model (Colotti *et al*. 2004). It is cleared that the general design guidance in the ACI, Triantafillou, and Colotti *et al*. models are derived from the experimental data and they are only applicable to external FRP reinforcement without anchorage. It is also important to take into consideration that all the ACI and Triantafillou models are semi empirical in nature, with important governing parameters derived from test data for beams strengthened with FRP laminates, whereas the ACI model cannot be applied in certain cases.

4.1 Analytical models

4.1.1 ACI model

The model proposed by the ACI Committee 440 (2000) is only applicable to RC beams externally reinforced with FRP materials. It is based on the classical formulation of shear strength for ordinary RC beams by adding the contribution of external shear reinforcement, that is

$$V_u = V_c + V_S + \gamma_f V_f \tag{1}$$

with

$$V_c = \left(1.9\sqrt{f_c'} + 2500\rho\frac{V_u d}{M_u}\right)b_w d \le 2\sqrt{f_c'}\,b_w d \tag{2}$$

$$V_s = \frac{A_{st} f_{ty} d}{s} \tag{3}$$

$$V_f = \frac{A_f E_f \varepsilon_{fe} d_f}{s_f} \tag{4}$$

In the above formulas, d is the effective depth of the beam section, $M_u/V_u d$ represents the shear span to depth ratio a/d, and $d_f = h_f - d'$ is the effective depth of the external reinforcement, d' being the concrete cover. Furthermore, ε_{fe} is the effective tensile strain in the FRP, E_f is the elastic modulus of FRP in the principal fiber orientation, and γ_f is a reduction factor equal to 0.95 for fully wrapped elements, and 0.85 for beams with two or three sides bonded. In Eq. (4), the effective FRP strain ε_{fe} is assumed to be smaller than the ultimate tensile elongation of the FRP composite ε_{fu}, depending on the governing mode of failure (related to the shear strengthening configuration) and can be computed as follows

$$\varepsilon_{fe} = \begin{cases} 0.004 \le 0.75\varepsilon_{fu} & \text{fully wrap ped} \\ k_v\varepsilon_{fu} \le 0.004 & \text{two to three sides bonded} \end{cases} \tag{5}$$

where

$$k_v = \frac{k_1 k_2 L_e}{11{,}900\varepsilon_{fu}} \le 0.75 \tag{6}$$

$$k_1 = \left(\frac{f_c'}{27}\right)^{2/3} \tag{7}$$

$$k_2 = \begin{cases} \dfrac{d_f - L_e}{d_f} & \text{fully wrap ped} \\ \dfrac{d_f - 2L_e}{d_f} & \text{two sides bonded} \end{cases} \tag{8}$$

$$L_e = \frac{23{,}300}{(t_f E_f)^{0.58}} \tag{9}$$

4.1.2 Triantafillou model

Triantafillou (1998) proposed a simple modeling approach for the evaluation of the shear capacity of strengthened RC members in which the contribution of externally bonded FRP shear reinforcement is calculated through equations obtained on a combination of qualitative arguments and calibration with experimental results. According to the Eurocode design format (EC2), the shear capacity V_u of a RC externally strengthened beam is given by

$$V_u = V_c + V_s + V_f \le 0.45 v_{ca} f_c' bd \tag{10}$$

with

$$V_c = \tau_R k(1.2 + 40\rho_l)bd \tag{11}$$

$$V_s = \frac{0.9 A_{st} f_{ty} d}{s} \tag{12}$$

Table 4 Comparison of results obtained with different models

Beam Designation	$V_{f,\exp}$ (kN)	$V_{f,\mathrm{ACI}}$ (kN)	$V_{f,\mathrm{Tri}}$ (kN)	$V_{f,\mathrm{col.}}$ (kN)
B2.7U90STA0	19.1	20.1	36.0	32.4
B2.7U90STA1	27.6	20.1	36.0	32.4
B2.7U90STA2	36.9	20.1	36.0	32.4
B2.7U90STA3	44.5	20.1	36.0	32.4

$$V_f = \frac{0.9A_f E_f \varepsilon_{fe} d}{s_f} \tag{13}$$

where τ_R=0.25f_{ct}, concrete shear resistance; f_{ct}=tensile strength of concrete; k=1.6-d≥1(d in m); ρ_l=A_{sl}/bd≤0.02; ρ_f=A_f/bs_f; v_{co}=0.7- $f_c^{/}$/200>0.5 ($f_c^{/}$ in MPa). The assumed equations for the effective FRP strain ε_{fe}, which are different (as in the ACI model) according to the shape as well as type of composite material used as external shear reinforcement, are as follows

$$\varepsilon_{fe} = \min \begin{cases} 0.00065\left(\dfrac{(f_c^{/})^{2/3}}{E_f \rho_f}\right)^{0.65} \\ 0.17\left(\dfrac{(f_c^{/})^{2/3}}{E_f \rho_f}\right)^{0.30} \varepsilon_{fu} \end{cases} \tag{14}$$

for beams with two to three sides bonded with CFRP

$$\varepsilon_{fe} = \min \begin{cases} 0.17\left(\dfrac{(f_c^{/})^{2/3}}{E_f \rho_f}\right)^{0.30} \varepsilon_{fu} \text{ for CFRP} \\ 0.048\left(\dfrac{(f_c^{/})^{2/3}}{E_f \rho_f}\right)^{0.47} \varepsilon_{fu} \text{ for AFRP} \end{cases} \tag{15}$$

In the above equations, $f_c^{/}$ is in MPa and E_f in GPa. Note that Eq. (14), calibrated for CFRP, should be used with caution for other types of FRPs.

4.1.3 Colotti et al. model

Colotti *et al*. (2004) presented a rational and systematic approach to predict the shear capacity of reinforced concrete beams strengthened by bonded external plates. The shear behavior of strengthened beams was modeled by the truss analogy method, in conjunction with the theory of plasticity. Compared to other current truss models, this proposed model considered also those failure modes influenced by bond slip, that is, the debonding phenomenon. In synthesis, the actual load carrying capacity of beams strengthened in shear was determined by the minimum value obtained from Eq. (16), where the total degree of shear reinforcement ψ=ψ_i+ψ_e takes the following expressions

$$\psi = \frac{A_s f_{ty}}{bsf_c^{/}} + \min\left(\frac{w_f h_f}{bs_f f_c^{/}} \tau_u ; \frac{2t_f w_f f_{fe}}{bs_f f_c^{/}}\right) \tag{16}$$

In deriving the model, it was implicitly assumed that the failure of the external reinforcement occurs after the yielding of the internal steel stirrups, according to the current design concept of the beams for which the steel yielding/concrete crushing occurs before FRP fracture or debonding failure.

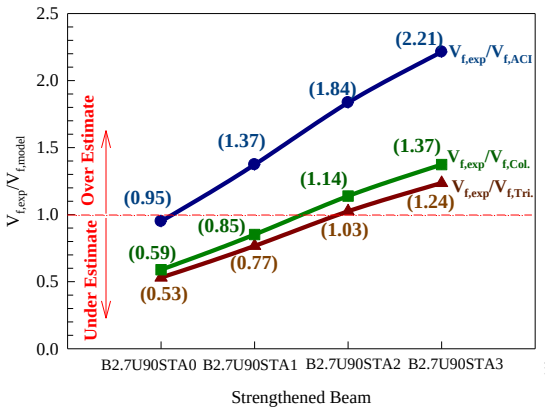

Fig. 9 The normalized experimental FRP shear force with respect to analytical models

4.2 Validation of experimental results with recent models

Table 4 shows a comparison of the results predicted by the three models $V_{f,\mathrm{ACI}}$ (ACI 2008), $V_{f,\mathrm{Tri}}$ (Triantafillou 1998), and $V_{f,\mathrm{Col.}}$ (Colotti *et al*. 2004). Fig. 9 shows a comparison of the results predicted by the three models $V_{f,\exp}/V_{f,\mathrm{ACI}}$ (ACI 2008), $V_{f,\exp}/V_{f,\mathrm{Tri}}$ (Triantafillou 1998), and $V_{f,\exp}/V_{f,\mathrm{Col.}}$ (Colotti *et al*. 2004). Note that the ACI and Triantafillou models were calibrated for CFRP, should be used with caution for other types of composites as shown in Fig. 9. The overall predictions by ACI model appear to be overestimated the ultimate capacity of the control beams without anchorage (B2.7U90STA0) with a percentage of 5% and underestimate the capacity of the anchorage beams with a percentage of 37%, 84%, 121% for B2.7U90STA1, B2.7U90STA2, and B2.7U90STA3, respectively. Also, Colotti *et al*. model appear to be overestimated the ultimate capacity of the control beams without anchorage (B2.7U90STA0) and the beam strengthened with 25 mm anchorage CFRP strips (B2.7U90STA1) with a percentage of 47% and 23%, respectively, as well as underestimate capacity of the anchorage beams with 50 mm (B2.7U90STA2) and 75 mm (B2.7U90STA3) CFRP strips with a percentage of 3% and 24% B2.7U90STA2 and B2.7U90STA3, respectively. In addition, Triantafillou *et al*. model appear to be overestimated the ultimate capacity of the control beams without anchorage (B2.7U90STA0) and the beam strengthened with 25 mm anchorage CFRP strips (B2.7U90STA1) with a percentage of 41% and 15%, respectively, as well as underestimate the capacity of the anchorage beams with 50 mm (B2.7U90STA2) and 75 mm (B2.7U90STA3) CFRP strips with a percentage of 14% and 37% B2.7U90STA2 and B2.7U90STA3, respectively. As a result, the overall predictions of ACI model appear to be underestimate the ultimate capacity of the tested beams with a mean $V_{f,\exp}/V_{f,\mathrm{ACI}}$ value of 1.59 and a coefficient of variation (COV) of 34% and the Colotti *et al*. model

overestimate the tested beams capacity with a mean $V_{f,\exp}/V_{f,\text{Col.}}$ value of 0.89 and a COV of 34%. While, Triantafillou *et al*. model shows the best agreement between the experimental and analytical ultimate load capacity with a mean $V_{f,\exp}/V_{f,\text{Tri.}}$ value of 0.99 and (COV) of 34%. Therefore, it's essential to consider the effect of anchorage on the shear behavior of RC beams strengthened externally with CFRP composites by adding a factor to the current proposed models.

5. Conclusions

Based on the experimental results, the following conclusions can be made:

- The use of CFRP composites is an effective technique to enhance the shear capacity of RC beams. The externally bonded CFRP can increase the shear capacity of the beam significantly by 15-34% than that the control beams, depending on the variables investigated.
- One of the observed failure modes was debonding of more than two CFRP strips due to debonding. Test results seem to indicate that this mechanism can be prevented by providing an anchoring the CFRP strips in the beam from top side.
- Bonded anchorage of CFRP strips with width of 0.1h-0.3h to the beam resulted in a decrease in average interface bond stress and an increase in the effective strain of the CFRP sheet at failure, which resulted in a higher shear capacity as compared with that of the U-wrapped beams without anchorage as well as delay or mitigate the sheet debonding from the concrete surface.
- The inclination of the primary shear crack influenced the shear strength contribution of the external strengthening. As was demonstrated in this study, the shear crack angle determined the number of CFRP strips intersected by the crack and whether or not an intersected CFRP strips was fully effective.
- The ACI model underestimated the ultimate capacity of the tested beams and the Colotti *et al*. model overestimated the tested beams capacity but Triantafillou *et al*. model shows the best agreement with the experimental and analytical ultimate load capacity.

Acknowledgements

The author acknowledges the technical support provided by Jordan University of Science and Technology.

References

ACI Committee 440 (2008), "Guide for the Design and Construction of Externally Bonded FRP Systems for strengthening Concrete Structures", ACI440.2R-08, American Concrete Institute; Farmington Hills, Mich.

Bianco, V., Barros, J.A.O. and Monti, G. (2010), "New approach for modeling the contribution of NSM FRP strips for shear strengthening of RC beams", *J. Compos. Constr.*, **14**(1), 36-48.

Bilotta, A., Ceroni, F., Di Ludovico, M., Nigro, E., Pecce, M. and Manfredi, G. (2011), "Bond efficiency of EBR and NSM FRP systems for strengthening concrete members", *J. Compos. Constr.*, **15**(5), 757-772.

Bousselham, A. and Chaallal, O. (2006), "Behaviour of reinforced concrete T-beams strengthened in shear with carbon fiber-reinforced polymer-an experimental study", *ACI Struct. J.*, **103**(3), 339-347.

Bousselham, A. and Chaallal, O. (2008), "Mechanisms of Shear Resistance of Concrete Beams strengthened in shear with externally bonded FRP", *J. Compos. Constr.*, **12**(5), 499-512.

Bukhari, I.A., Vollum, R.L., Ahmad, S. and Sagaseta, J. (2010), "Shear strengthening of reinforced concrete beams with CFRP", *Mag. Concrete Res.*, **62**(1), 65-77.

Cao, S.Y., Chen, J.F., Teng, J.G., Hao, Z. and Chen, J. (2005), "Debonding of RC beams shear strengthened with complete FRP wraps", *J. Compos. Constr.*, **9**(5), 417-428.

Ceroni, F. (2010), "Experimental performances of RC beams strengthened with FRP materials", *Constr. Build. Mater.*, **24**(1), 1547-1559.

Chaallal, O., Mofidi, A., Benmokrane, B. and Neale, K. (2011), "Embedded through-section FRP rod method for shear strengthening of RC beams: performance and comparison with existing techniques", *J. Compos. Constr.*, **15**(3), 732-742.

Chaallal, O., Nollet, M.J. and Perraton, D. (1998), "Shear strengthening of RC beams by externally bonded side CFRP strips", *J. Compos. Constr.*, **2**(2), 111-113.

Chen, J.F. and Teng, J.G. (2003), "Shear capacity of FRP-strengthened RC beams: FRP debonding", *Constr. Build. Mater.*, **17**(1), 27-41.

Colotti, V., Spadea, G. and Swamy, R.N. (2004), "Structural Model to Predict the Failure Behavior of Plated Reinforced Concrete Beams", *J. Compos. Constr.*, **8**(2), 104-122.

Deniaud, C. and Cheng, J.J.R. (2001), "Shear behaviour of reinforced concrete T-beams with externally bonded fiber-reinforced polymer sheets", *ACI Struct. J.*, **98**(3), 386-394.

Dias, S.J.E. and Barros, J.A.O. (2011), "Shear strengthening of RC T-section beams with low strength concrete using NSM CFRP laminates", *Cement Concrete Compos.*, **33**(2), 334-345.

Dias, S.J.E. and Barros, J.A.O. (2012), "NSM shear strengthening technique with CFRP laminates applied in high-strength concrete beams with or without pre-cracking", *Compos. Part B: Eng.*, **43**(2), 290-301.

Dias, S.J.E. and Barros, J.A.O. (2013), "Shear strengthening of RC beams with NSM CFRP laminates: experimental research and analytical formulation", *Compos. Struct.*, **99**(1), 477-490.

Galal, K. and Mofidi, A. (2010), "Shear strengthening of RC T-beams using mechanically- anchored unbonded dry carbon fibre sheets", *ASCE, J. Perform. Constr. Facil.*, **24**(1), 31-39.

Hojatkashani, A. and Kabir, M.Z. (2012), "Interfacial stress assessment at the cracked zones in CFRP retrofitted RC beams", *Struct. Eng. Mech.*, **44**(6), 12-23.

Hosen, M.A., Jumaat, M.Z., Islam, A.B.M.S., Kamruzzaman, M., Huda, M.N. and Soeb, M.R. (2015), "Eliminating concrete cover separation of NSM strengthened beams by CFRP end anchorage", *Struct. Eng. Mech.*, **56**(6), 36-47.

Jayaprakash, J., Samad, A.A.A., Abbasovich, A.A. and Ali, A.A. A. (2007), "Repair of precracked RC rectangular shear beams using CFRP strip technique", *Struct. Eng. Mech.*, **26**(2), 54-63.

Khalifa, A. and Nanni, A. (2000), "Improving shear capacity of existing RC T-section beams using CFRP composites", *Cement Concrete Compos.*, **22**(1), 165-174.

Khalifa, A. and Nanni, A. (2002), "Rehabilitation of rectangular simply supported RC beams with shear deficiencies using CFRP composites", *Constr. Build. Mater.*, **16**(3), 135-146.

Khalifa, A., Gold, W.J., Nanni, A, and Aziz, A., (1998), "Contribution of externally bonded FRP to shear capacity of RC flexural members", *J. Compos. Constr.*, **2**(2), 195-201.

Lee, H.K., Cheong, S.H., Ha, S.K. and Lee, C.G. (2011), "Behaviour and performance of RC T-section deep beams externally strengthened in shear with CFRP sheets", *J. Compos. Struct.*, **93**(1), 911-922.

Lee, H.K., Ha, S.K. and Afzal, M. (2008), "Finite element analysis of shear-deficient RC beams strengthened with CFRP strips/sheets", *Struct. Eng. Mech.*, **30**(2), 33-44.

Li, A., Assih, J. and Delmas, Y. (2001), "Shear strengthening of RC beams with externally bonded CFRP sheets", *J. Struct. Eng.*, **127**(4), 280-374.

Martinola, G., Meda, A., Plizzari, G.A. and Rinaldi, Z. (2010), "Strengthening and repair of RC beams with fiber reinforced concrete", *Cement Concrete Compos.*, **32**(1), 731-739.

Mofidi, A., Chaallal, O., Benmokrane, B. and Neale, K. (2012), "Performance of end-anchorage systems for RC Beams strengthened in shear with epoxy bonded FRP", *J. Compos. Struct.*, **16**(3), 322-331.

Mosallam, A.S. and Banerjee, S. (2007), "Shear enhancement of reinforced concrete beams strengthened with FRP composite laminates", *Compos. Part B*; **38**(1), 781-193.

Ozgur, A., Bulut, N. and Ayhan, M. (2012), "Strain distribution between CFRP strip and concrete at strengthened RC beam against shear", *Struct. Eng. Mech.*, **41**(4), 42-51.

Pannirselvam, N., Nagaradjane, V. and Chandramouli, K. (2009), "Strength behaviour of fiber reinforced polymer strengthened beams", *ARPN J. Eng. Appl. Sci.*, **4**(9), 34-39.

Pellegrino, C. and Modena, C. (2002), "Fiber reinforced polymer shear strengthening of reinforced concrete beams with transverse steel reinforcement", *J. Compos. Constr.*, **6**(2), 104-111.

Sato, Y., Katsumata, H. and Kobatake, Y. (1997), "Shear strengthening of existing reinforced concrete beams by CFRP sheet", *Proc. of the 3rd Int. Symp. on Non-Metallic (FRP) Reinforcement for Concrete Structures*, Sapporo, Japan.

Schuman, P. (2004), "Mechanical anchorage for shear rehabilitation of reinforced concrete structures with FRP: an appropriate design approach", Ph.D. Thesis. University of California. San Diego.

Seo, S., Feo, L. and Hui, D. (2013), "Bond strength of near surface-mounted FRP plate for retrofit of concrete structures", *Compos. Struct.*, **95**(1), 719-727.

Shuraim Ahmed, B. (2011), "Efficacy of CFRP configurations for shear of RC beams: experimental and NLFE", *Struct. Eng. Mech.*, **39**(3), 23-34.

Siddiqui, N.A. (2009), "Experimental investigation of RC beams strengthened with externally bonded FRP composites", *Lat. Am. J. Solid. Struct.*, **6**(1), 343-362.

Sundarraja, M.C. and Rajamohan, S. (2009), "Strengthening of RC beams in shear using GFRP inclined strips-an experimental study", *Constr. Build. Mater.*, **23**(1), 856-864.

Taljsten, B. (2003), "Strengthening concrete beams for shear with CFRP sheets", *Constr. Build. Mater.*, **17**(1), 15-26.

Teng, J.G., Lam, L. and Chen, J.F. (2004), "Shear strengthening of RC beams with FRP composites", *Prog. Struct. Eng. Mater.*, **6**(1), 173-184.

Triantafillou, T.C. (1998), "Shear strengthening of reinforced concrete beams using epoxy bonded FRP composites", *ACI Struct. J.*, **95**(2), 107-115.

Valerio, P., Bell, T.J. and Darby, A.P. (2009), "Deep embedment of FRP for concrete shear strengthening", *Proc ICE – Struct. Build.*, **162**(5), 311-321.

Zhang, Z. and Hsu, C.T.T. (2005), "Shear strengthening of reinforced concrete beams using carbon-fiber reinforced polymer laminates", *J. Compos. Constr.*, **9**(3), 158-69.